Bondareva et al., Supplemental section.

Isolation of *txnrd1* genomic clone and construction of targeting vector. A single *txnrd1* genomic clone of about 19 kb in length was isolated in a screen of 8 x 10^5 plaques from a mouse strain 129XI genomic library in a lambda-FIX II vector (Stratagene) using a [^{32}P]-labeled mouse Txnrd1 5' cDNA fragment [1] as probe. The full-length *Not* I/*Not* I insert was subcloned into a pBlueScript KS+ vector (Stratagene). The insert was restriction mapped and a 14-kb *Kpn* I/*Not* I sub-fragment that contained exons 1-5 was sequenced and used for production of the targeting vector (Fig. 1a)[1]. Briefly, the clone was cut with *Kpn* I, blunted with T4 DNA polymerase, and cut with *Not* I. The resultant 14-kb blunt/*Not* I fragment was inserted into TK1-TK2C vector [2] that had been cut with *Xho* I, filled with Klenow, and cut with *Not* I, thus flanking the insert with an expressed HSV-*tk* gene for use in positive/negative selection [2, 3]. The *lox*P-flanked MC1-neo selectable marker cassette was amplified by PCR using the KT1LoxA plasmid as template [4] and primers Neo-5' and Neo/LoxP-3' (Table S1). The PCR product was digested with *Sal* I and ligated into the unique *Xho* I site in the *txnrd1* insert, thereby killing the site, and a clone bearing the correct orientation was selected based on the asymmetric *Xba* I site (Fig. 1a). The downstream co-linearly-oriented *lox*P site was inserted by annealing equimolar amounts of primers LoxP-Bgl2-5' and LoxP-Bgl2-3' (Table S1), ligating the annealed product into the unique *Bam* HI site (thereby killing the site), and screening for correct orientation by sequencing. All cloning junctions in the final targeting vector were confirmed by sequencing.

The targeting vector was linearized with *Not* I and was electroporated into mouse strain 129XI ES cells. G418/ganciclovir double-resistant clones (144 total) were isolated, expanded, and split into two cultures; one of which was used for genomic DNA production and one of which was frozen. Genomic DNA was digested with *Xba* I and analyzed by Southern blotting (Fig. S1a) using the *Xba* I/*Kpn* I probe shown in Fig. 1a. Clones containing a targeted insertion of the upstream *lox*P-MC1-neo marker at the *Xho* I site (59 of 144) were screened by amplifying across the *Bam* HI site by radioactive PCR for the downstream *lox*P site using primers Txnrd1-D and -E (Fig. 1a, Table S1), resolving the products on a 6.5% polyacrylamide/8 M urea sequencing gel, and exposing the dried gel to X-ray film (Fig. S1b). Eight of the 59 neo-targeted clones also bore a *lox*P site at *Bam* H1; one of these was chosen for mouse production.

ES cells from the selected clone were used for chimeric mouse production by injection into C57Bl/6J blastocysts. Highly chimeric phenotypically male pups were bred to C57Bl/6J dams and genomic DNA samples were isolated from agouti pups. Genotype was determined by PCR using primers Txnrd1-B, -C, and -G (Figs 1a, 1b, Table S1, and data not shown), and pups bearing the targeted allele were selected for subsequent husbandry. These pups were heterozygous for the conditional (*txnrd1*^{cond}) allele; the line has since been extensively backcrossed to C57Bl/6J animals to produce a line with the conditional allele on a homogeneous C57Bl/6J background. Animals from this colony were crossed to members of our colony of the "deleter" strain of mice, which bear an X chromosome-linked *Cre*-transgene [5] to generate the *txnrd1*$^{-}$ line. These mice have now been back-crossed onto C57Bl/6J more than ten generations. No changes in phenotype have been observed as a result of back-crossing (not shown).

In situ hybridizations. Probes for *in situ* hybridizations were transcribed with the following enzymes and templates: Brachyury (t), 284 bp partial cDNA clone extending from position 1763 – 2046 (NCBI accession # X51683) in pBlueScript KS, linearized with *Bam* HI and transcribed

with T3 RNA polymerase (RNAP) [6]. Cripto, 983 bp partial cDNA clone extending from position 41 – 1024 (NCBI accession # NM_011562) in pBluescript II KS+, linearized with *Hind* III and transcribed with T7 RNAP [7]. Lim1, 2.17 kb partial cDNA from position 370 – 2543 (NCBI accession # NM_008498) cloned into plasmid pBluescript KS-, linearized with *Hind* III and transcribed with T7 RNAP [8]. Fgf8, 699 bp partial cDNA from position 39 – 738 (NCBI accession # U18673) in plasmid pGem92F-, linearized with *Hind* III and transcribed with T7 RNAP [9]. Snail1, 470 bp partial cDNA (NCBI accession # NM_011427) in pGEM7 2f+, linearized with *Bam* HI and transcribed with T7 RNAP [10].

Transcription reactions for generating digoxygenin-labeled probes used 2.5 µg of the linearized templates indicated above and the corresponding RNAP from either Promega or New England Biolabs with the corresponding manufacturer's buffer, in 50 µl reactions containing 0.5 mM ATP, CTP, and GTP; 0.33 mM UTP; 0.17 mM digoxygenin-11-UTP (Roche); 20 µCi alpha-[^{32}P]CTP (800 Ci/mmol); and 1 U/µl RNasin (Promega). Reactions were incubated 2 h at 37^{o}C and then each received 200 µg yeast RNA and 2.5 U RNase-free DNase (Fisher). Incubation was continued at 37^{o}C for 20 min and reactions were stopped by adding 130 µl of a buffer containing 1% SDS, 20 mM EDTA, 20 mM Tris, pH 7.5, and 100 mM NaCl. Samples were desalted on Sephadex G-50-fine columns in the same buffer. Probe yield was calculated from percent incorporation of radio-labeled CTP.

Embryos from timed matings between *txnrd1*$^{-/+}$ parents were harvested at E7.5 or E8.5 into ice-cold PBST (PBS containing 0.1% Tween-20). After harvest, embryos were fixed overnight at 4^{o}C in PBST containing 4% paraformaldehyde, washed in PBST, and serially dehydrated into 100% methanol. Embryos from multiple age-matched litters were pooled and groups of about 12 embryos (typically from 2-3 litters) were processed for each probe.

Embryos were serially rehydrated into PBST and were incubated 2 h at room temperature in PBST containing 6% H_2O_2. They were washed 3 times with PBST and then incubated 5 min at room temperature in PBST containing 10 µg/ml proteinase K. Embryos were washed 2 times with 2 mg/ml glycine in PBST followed by two washes with PBST. Embryos were re-fixed for 20 min at room temperature in 4% paraformaldehyde, 0.2% glutaraldehyde in PBST and washed 3 times in PBST. Embryos were pre-hybridized for 2 h at 65^{o}C in hybridization buffer (50% formamide, 1X Denhardt's, 5X SSC, 1% SDS, 50 µg/ml heparin, 50 µg/ml yeast RNA) and were then hybridized overnight at 65^{o}C in hybridization buffer containing 0.5 µg/ml of digoxygenin-labeled RNA probe. Embryos were then washed twice for 30 min at 65^{o}C in solution I (50% formamide, 5X SSC, 1% SDS), once for 10 min at 65^{o}C in 50% solution I, 50% solution II (0.5 M NaCl, 10 mM Tris-Cl, pH. 7.5, 0.1% Tween-20), 3 times for 5 min at room temperature in solution II, and incubated 1 hr at 37^{o}C in solution II containing 100 µg/ml RNase A and 100 U/ml RNase T1. Embryos were washed twice for 30 min at 65^{o}C in solution III (50% formamide, 2X SSC) and 3 times for 5 min at room temperature in TBST (10 mM Tris, pH 7.5, 137 mM NaCl, 2.7 mM KCl, 0.1% Tween-20). Embryos were blocked in TBST containing 10% sheep serum at room temperature for 2.5 h and incubated at 4^{o}C overnight in TBST containing 10% sheep serum and a 1:2,000 dilution of alkaline phosphatase-conjugated anti-digoxygenin Fab fragment (Roche) that was pre-adsorbed against mouse embryo acetone extract. The next day, embryos were washed 3 times for 5 min at room temperature in TBST, 6 times for 1 h at room temperature in TBST, and twice for 20 min in AP buffer (100 mM Tris, pH 9.5, 50 mM $MgCl_2$, 100 mM NaCl, 0.1% Tween-20). Embryos were then incubated in AP buffer containing 337 µg/ml nitro blue tetrazolium (NBT, Fisher) and 175 µg/ml 5-bromo-4-chloro-3-indolyl

phosphate p-toluidine (BCIP, Fisher) and color reaction was allowed to develop 2-16 h, as optimized for each probe. Color development reactions were stopped by placing embryos in PBST containing 5 mM EDTA. Embryos were re-fixed in PBST containing 4% paraformaldehyde for 4 h at room temperature and washed twice for 5 min in PBST containing 5 mM EDTA and were serially dehydrated into 100% methanol. Embryos were serially rehydrated into PBST containing 5 mM EDTA and were then serially equilibrated into 4:1 glycerol:PBST mixture.

Embryos were segregated into separate vials, individually labeled, and photographed. For subsequent genotyping, each embryo was transferred into a labeled tube containing 10 µl of digestion solution (50 mM Tris, pH 7.5, 100 mM NaCl, 100 mM EDTA, 1% SDS, 100 µg/ml proteinase K) and incubated at 52^{o}C overnight. Samples were diluted to 100 µl with 1 mM Tris, pH 7.5, 0.5 mM EDTA, 0.1% SDS, 250 mM NaCl, extracted with an equal volume of phenol/chloroform/isoamyl alcohol (25:24:1) and nucleic acids were precipitated with 300 µl ethanol. Nucleic acids were resuspended in 20 µl TE and 0.5 µl was used in radio-labeled PCR genotyping reactions (Fig. 1c).

Single-embryo cDNA production, RT-PCR, real-time PCR, and oligonucleotide array analyses. Pregnant uteri were harvested into ice-cold PBS; embryos were dissected out and placed into individual 0.5 ml tubes containing 10 µl 1X TES (10 mM Tris, pH 7.5, 5 mM EDTA, 1% SDS) with 100 µg/ml proteinase K. Tubes were sealed and incubated 2-20 hours at 52^{o}C. Samples received 90 µl of 0.1X TES, 5 µl of 5 M NaCl, were extracted with an equal volume of phenol/choloroform/isoamyl alcohol (25:24:1) followed by pure chloroform, and were precipitated with 300 µl ethanol at -20^{o}C overnight. Nucleic acid was precipitated and resuspended in 10 µl water. A portion (1-3 µl) was used for radioactive PCR-based genotypic analyses (Fig. 1c), and the remainder was used for cDNA production. All samples used for either RT-PCR or array analyses had been molecularly genotyped as shown in Fig. 1c.

For cDNA production, total nucleic acid from the embryos (typically 75% of the embryo) was used with the two-cycle cDNA synthesis system (Affymetrix) using the manufacturer's recommended conditions. For RT-PCR and real-time PCR analyses (see below) cDNAs were diluted 10-fold with water. For oligonucleotide array analyses, cDNAs were transcribed to produce biotin-labeled cRNA probes using the IVT reaction system (Affymetrix) by the manufacturer's recommended protocols.

cRNA probes were fragmented and were hybridized to mouse oligonucleotide gene expression arrays (Affymetrix, version 430-2.0) by the manufacturer's recommended protocols. Arrays were read by an Affymetrix array reader and data from all six arrays were analyzed statistically using GeneSpring (Agilent), as described in text. Data included in tables met the following criteria: 1) upon averaging data over the three pair of littermate embryos (six arrays), signals were consistent enough to give a P-value ≤ 0.05; 2) sequences on which probe set was based were annotated by Affymetrix or could be annotated with GeneSpring or BLAST. In addition, for Tables 2 and 3, the average abundance of each mRNA differed by $\geq$ 3-fold between wild-type and mutant embryos.

For single embryo PCR-based verification reactions, litters were harvested from timed matings between *txnrd1*$^{-/+}$ parents at E7.5, nucleic acids were extracted, and genotypes were determined as described above. cDNAs were prepared from *txnrd1*$^{+/+}$ and *txnrd1*$^{-/-}$ embryos as described above and each was resuspended in 50 µl of water per embryo. For semi-quantitative

analyses, six identical standard PCR reaction mixes were prepared on ice containing 0.5 µl of cDNA and 0.2 pmol/µl each of the indicated primers (see figure legends, Table S1) in a standard PCR reaction mix, thermal-cycling was begun on all samples and individual tubes were removed and stopped by adding 1 µl 0.5 M EDTA and chilling on ice at sequential intervals depending on the empirical abundance of each mRNA. Samples were subjected to agarose gel electrophoresis and products were visualized by ethidium bromide staining. For real-time PCR analyses, reaction mixes were similar, but contained a 1:2 x 10^5 dilution of SYBR green solution (Invitrogen). Real-time PCR reactions were performed in a Perkin-Elmer 5700 machine and associated software was used for data analysis and presentation.

Because our goal was to use these cDNA samples as templates to generate probes for hybridization to oligonucleotide microarrays, we needed a means to evaluate the quality and comparability of each cDNA. As a first test, we evaluated the degree of 3'-bias in each sample by semi-quantitative PCR on ubiquitously expressed abundant (β-actin, ~ 10^3 mRNA molecules per cell) and rare (TATA-binding protein, TBP, <10 mRNA molecules per cell)[11] mRNAs (Fig. S2a). Our rationale was that decreases in RNA quality (i.e., endonucleolytic nicks) would un-tether 5' mRNA sequences from the poly(A) tail, resulting in an increase in the 3'-bias of the cDNA pool; comparable samples would have similar 5':3' ratios. Semi-quantitative PCR results showed similar 5':3' ratios for β-actin and for TBP (Fig. S2a). As a second test, we generated biotinylated cRNAs from six single embryo cDNAs (mutant and wild-type littermate pairs from three E7.5 litters), and hybridized each to a mouse oligonucleotide expression array. Raw hybridization signal data were analyzed for seven ubiquitously expressed housekeeping mRNAs whose expression levels varied over roughly a 1000-fold range (Fig. S2b). Results showed uniform hybridization signals for all seven mRNAs both within a genotype (represented by standard deviation on bars) and between the genotypes (compare wild-type and mutant bar heights). Finally, real-time PCR analyses for representative mRNAs using single-embryo *txnrd1*$^{+/+}$ and *txnrd1*$^{-/-}$ cDNA preparations showed product accumulation curves that matched array data and first-derivative melting curves that matched expected melting temperatures based on G/C content (Fig. S2c). We concluded that this approach provided reliable mRNA abundance profiles for mRNAs expressed at a wide range of levels in individual E7.5 embryos.

FOOTNOTES

[1]For all tables and figures, the prefix "S" indicates reference to an exhibit in the supplemental section; lack off a prefix indicates reference to an exhibit in the main text.

REFERENCES

[1] Sun, Q. A., Kirnarsky, L., Sherman, S., and Gladyshev, V. N. Selenoprotein oxidoreductase with specificity for thioredoxin and glutathione systems. *Proc Natl Acad Sci U S A* **98***:*3673-3678; 2001.

[2] Mansour, S. L., Thomas, K. R., and Capecchi, M. R. Disruption of the proto-oncogene int-2 in mouse embryo-derived stem cells: a general strategy for targeting mutations to non-selectable genes. *Nature* **336***:*348-352; 1988.

[3] Thomas, K. R., and Capecchi, M. R. Targeted disruption of the murine int-1 proto-oncogene resulting in severe abnormalities in midbrain and cerebellar development. *Nature* **346***:*847-850; 1990.

[4] Deng, C., Thomas, K. R., and Capecchi, M. R. Location of crossovers during gene targeting with insertion and replacement vectors. *Mol Cell Biol* **13***:*2134-2140; 1993.
[5] Gu, H., Zou, Y. R., and Rajewsky, K. Independent control of immunoglobulin switch recombination at individual switch regions evidenced through Cre-loxP-mediated gene targeting. *Cell* **73***:*1155-1164; 1993.
[6] Herrmann, B. G., Labeit, S., Poustka, A., King, T. R., and Lehrach, H. Cloning of the T gene required in mesoderm formation in the mouse. *Nature* **343***:*617-622; 1990.
[7] Dono, R., Scalera, L., Pacifico, F., Acampora, D., Persico, M. G., and Simeone, A. The murine cripto gene: expression during mesoderm induction and early heart morphogenesis. *Development* **118***:*1157-1168; 1993.
[8] Barnes, J. D., Crosby, J. L., Jones, C. M., Wright, C. V., and Hogan, B. L. Embryonic expression of Lim-1, the mouse homolog of Xenopus Xlim-1, suggests a role in lateral mesoderm differentiation and neurogenesis. *Dev Biol* **161***:*168-178; 1994.
[9] MacArthur, C. A., Shankar, D. B., and Shackleford, G. M. Fgf-8, activated by proviral insertion, cooperates with the Wnt-1 transgene in murine mammary tumorigenesis. *J Virol* **69***:*2501-2507; 1995.
[10] Smith, D. E., Franco del Amo, F., and Gridley, T. Isolation of Sna, a mouse gene homologous to the Drosophila genes snail and escargot: its expression pattern suggests multiple roles during postimplantation development. *Development* **116***:*1033-1039; 1992.
[11] Schmidt, E. E., and Schibler, U. High accumulation of components of the RNA polymerase II transcription machinery in rodent spermatids. *Development* **121***:*2373-2383; 1995.
[12] Schmidt, E. E., and Schibler, U. Cell size regulation, a mechanism that controls cellular RNA accumulation: consequences on regulation of the ubiquitous transcription factors Oct1 and NF-Y and the liver-enriched transcription factor DBP. *J Cell Biol* **128***:*467-483; 1995.

FIGURE LEGENDS

Fig. S1, Identification of targeted ES cell clones. *a,* Southern blot of ES cell clones using *Xba* I-cut genomic DNA and the *Xba* I/*Kpn* I probe indicated in Fig. 1a. Selected clone identities are indicated above and positions of diagnostic bands are indicated at left. Of the 144 clones isolated, 59 (41%) bore a neo-targeted *txnrd1* allele. *b,* analysis for downstream *lox*P site. Diagnostic PCR using primer set D-E (Fig. 1a, Table S1) was used to determine which neo-targeted clones also contained the downstream *lox*P site. Eight of the 59 clones (6 of 46 clones shown on autoradiogram; 14% of neo-targets) bore the downstream *lox*P site.

Fig. S2, Assay verification for single embryo mRNA abundance analyses. *a,* RT-PCR cDNA quality control by analysis of 3':5' ratio for abundant (β-actin, ~10^3 mRNA molecules per cell) and rare (TBP, <10^1 mRNA molecules per cell) housekeeping mRNAs [11, 12]. *b,* raw normalized microarray hybridization signals for representative housekeeping genes whose basal mRNA abundances differ across a 10^3-fold range. Data points represent average $\pm$ 1 s.d. from three wild-type and three mutant E7.5 embryos, each analyzed on a separate microarray. *c,* real-time RT-PCR data quality for malic enzyme mRNA (Mod1), β-actin mRNA, and Fgf13 mRNA. At left is the plot of fluorescence (log scale, arbitrary units) per cycle (cycles 1-36 plotted). At right is a first derivative plot of the melting curve over a linear range from 60 – 95°C. The peak for the Mod1 PCR product, which was A/T-rich, was at 70.5°C; both β-actin and Fgf13 peaks

were at 87.0^{o}C. Abbreviations: ATP5b, ATP synthase β-chain precursor; Cycs, somatic cell cytochrome C; Eif2s2, translation initiation factor 2 subunit 2; Fgf13, fibroblast growth factor family member 13; Gapdh, glyceraldehyde-3-phosphate dehyrogenase; L7, large ribosomal subunit protein 7; Mod1, malic enzyme; TBP, TATA-binding protein.

Table S1. Oligonucleotide primer sequences

name	sequence
Cbr3-3’ Forward	5’-gtgacagtccttacgaggatcctg-3’
Cbr3-3’ Reverse	5’-tattgatcaaagcaggcacattaactggttg-3’
Cdh2-3' Forward	5'-tatggatccagatactgtggagcctgatgc-3'
Cdh2-3' Reverse	5'-tatgaattcgcacggtgctagtggactacag-3'
Fgf13-3' Forward	5’-ccatttagatcttcatatctgttgcatgg-3’
Fgf13-3' Reverse	5’-tatgaattcggtgcgtatttgggtatacaac-3’
Gclm1-3' Forward	5’-tatctcgagacatacagctactgactcacaatg-3’
Gclm1-3' Reverse	5’-tatagatctagaatacagtggttcctgtgagc-3’
Gstμ1-3' Forward	5'-tatctcgagctcactaggaggacctgtccac-3'
Gstμ1-3' Reverse	5'-tatgaattcgacagacctggggaggctactcc-3'
Igfbp1-3' Forward	5’-tatctcgagctggactctgctggtgtgtcta-3’
Igfbp1-3' Reverse	5’-tatgaattctggttacacaatcagcatcggaac-3’
LoxP-Bgl2-3’	5’-gatctataacttcgtatagcatacattatacgaagttata-3’
LoxP-Bgl2-5’	5’-gatctataacttcgtataatgtatgctatacgaagttata-3’
Mash2-3' Forward	5'-tatggatcctactcgtcggaggaaagcagctg-3'
Mash2-3' Reverse	5'-tatgaattctgtagagtcctacaacagttcaag-3'
Mod1-3’ Forward	5’-tatagatctaattatgaccagatcctacctga-3’
Mod1-3’ Reverse	5’-tatctcgagcttcctacatatcagtgaggac-3’
Neo/LoxP-3’	5’-acgcgtcgacataacttcgtataatgtatgctatacgaagttatgg-3’
Neo-5’	5’-acgcgtcgacggatcttccgatgtcgagcagtg-3’
Nodal-3’ Forward	5’-tatctcgagtggtctgtgacctgctgtccctc-3’
Nodal-3’ Reverse	5’-tatagatctgccaagcatacatctcaggact-3’
Oligo(dT)-T7	5’-ggccagtgaattgtaatacgactcactatagggaggcgg$(t)_{24}$-3’
Pcdh8-3' Forward	5'-tatagatctgacagtgactcggacatcagcgg-3'
Pcdh8-3' Reverse	5'-tatgaattctgaaaccgggtcaataacttag-3'
Pl1-3’ Forward	5’-tatgaattctggagggacttcaga-3’
Pl1-3’ Reverse	5’-tatagatcttatggatgtccctttta-3’
Prdx1-3’ Forward	5’-tgggcagaccaatcttctatcagtcac-3’
Prdx1-3’ Reverse	5’-taggcaggtagatctttcagaggcca-3’
Prdx2-3’ Forward	5’-tctggtgaatagtgatcctgccctga-3’
Prdx2-3’ Reverse	5’-catgtctatgcacgttctgcccatgt-3’
Prdx4-3’ Forward	5’-gactgactatcgtgggaaatacttgg-3’
Prdx4-3’ Reverse	5’-cacaatgacctttattgagaaggtcc-3’
Sox11-3’ Forward	5’-tatggatccgactactgcacgccggagctg-3’
Sox11-3’ Reverse	5’-tatgaattcgtaacagttgtgccgccaaaagg-3’
Srxn1-3’ Forward	5’-tgcaaacctagagtccaggaggcaat-3’
Srxn1-3’ Reverse	5’-gaaaagttgcagagactagagttccc-3’
t-3’ Forward	5’-atcctggaattcgtccacccccctgt-3’
t-3’ Reverse	5’-tatagatctgcagattgtctttggctactttg-3’
TBP-3’ Forward	5’-ggaaggccttgtgctgacccaccagc-3’
TBP-3’ Reverse	5’-gctagcggccgcccaagtagcagcacagagc-3’
TBP-5’ Forward	5’-atcgtcgactatggaccagaacaacagccttcca-3’

TBP-5’ Reverse	5’-atagcggccgcttaagagctctcagaagctggtgtggca-3’
Txnrd1 A	5’-tatggatcctcagtttgcttccgtcag-3’
Txnrd1 B	5’-caacagattgcatgctcttgg-3’
Txnrd1 C	5’-tatactagtgtcttggagggacgtgaagcag-3’
Txnrd1 D	5’-tatactagtgctggtcttggattttgtcac-3’
Txnrd1 E	5’-ctgctgaacctaaatctacagcactg-3’
Txnrd1 F	5’-atagaattccaaggcgacataggatgcac-3’
Txnrd1 G	5’-tatactagtcatagccgaatagcctct-3’
TxnRd2-3' Forward	5'-tatggatccatactggacggcaaaccagagct-3'
TxnRd2-3' Reverse	5'-tatgaattcgatttccaatgttgtgaatacctc-3'
TxnRd3-3' Forward	5'-tatggatccagtaccaaccctaagaatcag-3'
TxnRd3-3' Reverse	5'-gatgaattctgtctgcatcacctgtgcatatg-3'
Wnt5a-3’ Forward	5’-tatgaattcatttcccctcagctacaatg-3’
Wnt5a-3’ Reverse	5’-tattgatcacacaagacagaaatatgtacat-3’
βactin-3' Forward	5’-gctgtctggtggtaccaccatgta-3’
βactin-3' Reverse	5’-atctgctggaaggtggacagtgag-3’
βactin-5' Forward	5’-acgatatcgctgcgctggtcgtcg-3’
βactin-5' Reverse	5’-tggggtacttcagggtcaggatac-3’

Table S2. Cell cycle- and proliferation-dependent mRNA levels.

mRNA[1]	difference[2]	P-value[3]	description	GenBank
Ccnd2	-11.4	0.03	cyclin D2	NM_009829
Ccnd2	-10.9	0.02	cyclin D2	BQ175880
Ccnd2	-8.2	0.02	cyclin D2	AK007904
Ccnd2	-7.7	0.03	cyclin D2	NM_009829
Ccnd1	-4.0	0.05	cyclin D1	NM_007631
Ccnd2	-2.8	0.05	cyclin D2	NM_009829
Ccnd1	-2.6	0.04	cyclin D1	NM_007631
Ccnd2	-1.7	0.02	cyclin D2	NM_009829
Ccni	-1.7	0.02	cyclin I	NM_017367
Cdk2	-1.7	0.02	cyclin-dependent kinase 2	NM_016756
Cks2	-1.6	0.02	CDC28 protein kinase regulatory subunit 2	NM_025415
Ccni	-1.5	0.01	cyclin I	NM_017367
Cdk7	-1.4	0.01	cyclin-dependent kinase 7	U11822
Cdk8	-1.4	0.01	cyclin-dependent kinase 8	BC025046
Cdk4	-1.3	0.01	cyclin-dependent kinase 4	NM_009870
Pold1	-1.2	0.05	DNA pol, delta 1, catalytic subunit	BC009128
Rrm1	-1.2	0.04	ribonucleotide reductase M1	BB758819
Polb	-1.2	0.05	DNA pol, beta	BG094331
Mcm2	-1.2	0.05	minichromosome maintenance deficient 2	NM_008564
Mcm4	-1.2	0.04	minichromosome maintenance deficient 4	BC013094
Cks2	-1.2	0.01	CDC28 protein kinase regulatory subunit 2	NM_025415
Pole3	-1.2	0.04	DNA pol epsilon, subunit 3	AK007693
Ccne2	-1.2	0.01	cyclin E2	AF091432
Ccng2	-1.2	0.03	cyclin G2	U95826
H2av	-1.1	0.05	H2A histone family, member V	BC028539
Dhfr	-1.1	0.03	dihydrofolate reductase	AK018462
H2afz	-1.1	0.02	H2A histone family, member Z	AY074806
H2afy3	-1.1	0.03	H2A histone family, member Y2	NM_026230
Polb	-1.1	0.02	DNA pol, beta	BG094331
Mcm8	-1.1	0.02	minichromosome maintenance deficient 8	AK010365
Pold1	-1.1	0.03	DNA pol, delta 1, catalytic subunit	BC009128
Cdk4	-1.1	0.00	cyclin-dependent kinase 4	NM_009870
Lig1	-1.1	0.02	DNA ligase 1, ATP-dependent	NM_010715
Polr2k	-1.1	0.01	RNA pol II, polypeptide K	AA175187
Cdk9	-1.1	0.01	cyclin-dependent kinase 9	NM_130860
Hdac5	-1.1	0.02	histone deacetylase 5	NM_010412
Myst3	-1.1	0.04	MYST histone acetyltransferase 3	BF468324
Ccnt2	-1.1	0.03	cyclin T2	AK013634
Recc1	-1.1	0.01	replication factor C 1	U01222
Pole2	-1.1	0.01	DNA pol, epsilon 2 (p59 subunit)	AF036898
Prim1	-1.1	0.02	DNA primase, p49 subunit	J04620
Orc6l	-1.1	0.01	origin recognition complex, subunit 6-like	NM_019716
Hist1h3a	-1.1	0.02	histone 1, H3a	NM_013550 (1h4h)
Chrac1	-1.1	0.02	chromatin accessibility complex 1	NM_053068
Blm	-1.1	0.02	Bloom syndrome homolog	NM_007550
Polr3d	-1.1	0.04	RNA pol III, polypeptide D	BC016102
Ccnh	-1.1	0.02	cyclin H	NM_023243
Polr2g	-1.1	0.01	RNA pol II, polypeptide G	NM_026329
Ccna2	-1.1	0.02	cyclin A2	X75483
Polk	-1.1	0.03	DNA pol, kappa	BC008105
Cdk4	-1.1	0.05	cyclin-dependent kinase 4	NM_009870
Rfc5	-1.1	0.03	replication factor C (activator 1) 5	AK011489

Poldip2	1.0	0.04	DNA pol, delta interacting protein 2	NM_026389
Orc1l	1.0	0.02	origin recognition complex, subunit 1-like	BC015073
Polr2i	1.0	0.01	RNA pol II, polypeptide I	BB284638
Ccnb2	1.0	0.00	cyclin B2	AK013312
Rpa2	1.0	0.01	replication protein A2	BC004578
Cdk5	1.0	0.00	cyclin-dependent kinase 5	NM_007668
Orc4l	1.0	0.01	origin recognition complex, subunit 4	AK011550
Ccne1	1.0	0.01	cyclin E1	NM_007633
H3f3a	1.0	0.01	H3 histone, family 3A	BB252350
Prim1	1.0	0.01	DNA primase, p49 subunit	J04620
Ccna2	1.0	0.01	cyclin A2	X75483
Poldip3	1.0	0.01	DNA pol, delta interacting protein 3	AK003596
H2afz	1.0	0.05	histone H2A.Z	AV215230
Ccnh	1.0	0.01	cyclin H	NM_023243
Polg2	1.0	0.04	DNA pol, gamma 2, accessory subunit	NM_015810
Pole	1.0	0.01	DNA pol, epsilon	NM_011132
Pttg1	1.0	0.04	pituitary tumor-transforming 1	AF069051
Poldip3	1.0	0.01	DNA pol, delta interacting protein 3	BB534975
Poldip3	1.0	0.01	DNA pol, delta interacting protein 3	BI963573
Pole4	1.1	0.03	DNA pol, epsilon 4 (p12 subunit)	BF577544
Tyms	1.1	0.02	thymidylate synthase	BC020139
Hist1h3a	1.1	0.02	histone 1, H3a	NM_013550
Poldip2	1.1	0.03	DNA pol, delta interacting protein 2	NM_026389
Polb	1.1	0.03	DNA pol, beta	BC006681
Myst2	1.1	0.03	MYST histone acetyltransferase 2	BM225168
Hdac6	1.1	0.03	histone deacetylase 6	NM_010413
Pole4	1.1	0.05	DNA pol, epsilon 4 (p12 subunit)	BF577544
Poldip3	1.1	0.03	DNA pol, delta interacting protein 3	BB377698
Prim2	1.1	0.03	DNA primase, p58 subunit	NM_008922
Ccnf	1.2	0.01	cyclin F	NM_007634
Cdkn1a	1.2	0.04	cyclin-dependent kinase inhibitor 1A (p21)	AK007630
Pola2	1.2	0.03	DNA pol, alpha 2	NM_008893
Hirip5	1.2	0.04	histone cell cycle interacting protein	BC018355
Cdk5	1.4	0.03	cyclin-dependent kinase 5	NM_007668
Ccnd3	1.6	0.04	cyclin D3	NM_007632
Cdkn1c	2.0	0.00	cyclin-dependent kinase inhibitor 1C (p57)	NM_009876

[1] mRNAs having multiple entries were represented by more than one oligonucleotide probe set on the arrays and thus provided independent data readouts. In some cases, probe sets were designed from different GenBank files; in other cases they were designed to a common GenBank file, as indicated in right column. [2] Only mRNAs in which the higher signal was $\geq$ 200 units were included. [3] All data based on statistical analysis of individual arrays from three wildtype and mutant littermate pairs using GeneSpring softwear; only mRNAs showing sufficient signal reproducibility between the three paired array sets to yield a P-value $\leq$ 0.05 were included.

Table S3, Oxidoreductase mRNA levels

mRNA[1]	difference	P-value	description	GenBank	Notes
Npn3 (Srxn1)	10.9	0.00	neoplastic progression 3 (sulfiredoxin 1)	BM210600	
Cbr3	4.9	0.01	carbonyl reductase 3	AK003232	
Ltb4dh	4.3	0.00	leukotriene B4 12-dehydrogenase	BC014865	
Blvrb	3.5	0.00	biliverdin reductase B	BC027279	
Mod1	3.3	0.00	malic enzyme, supernatant	BC011081	
Mod1	3.2	0.03	malic enzyme, supernatant	AK006387	
Gpx3	2.5	0.01	glutathione peroxidase 3	NM_008161	
Ehhadh	2.1	0.01	enoyl-Co A, hydratase/3-hydroxyacyl Co A dehydrogenase	NM_023737	
Cox5a	1.2	0.04	cytochrome c oxidase, subunit Va	NM_007747	
Akr1a4	1.2	0.04	aldo-keto reductase 1 A4	AK009462	
Sc5d	1.1	0.05	sterol-C5-desaturase homologue	AB016248	
Idh3g	1.1	0.04	isocitrate dehydrogenase 3 (NAD+), gamma	NM_008323	
Ndufa5	1.1	0.04	NADH dehydrogenase 1 alpha subcomplex, 5	NM_026614	
Ndufa5	1.1	0.03	NADH dehydrogenase 1, alpha subcomplex, 5	NM_026614	
Ndufab1	1.1	0.04	NADH dehydrogenase 1, alpha/beta subcomplex, 1	AK010307	
Cox8a	1.1	0.03	cytochrome c oxidase, subunit VIIIa	NM_007750	
Phgdh	1.1	0.04	3-phosphoglycerate dehydrogenase	L21027	
Cox5b	1.1	0.02	cytochrome c oxidase, subunit Vb	NM_009942	
Aldh7a1	1.1	0.02	aldehyde dehydrogenase family 7A1	BC012407	
Uqcrb	1.1	0.03	ubiquinol-cytochrome c reductase binding protein	NM_026219	
Np15	1.1	0.02	nuclear protein 15.6	BC027265	
Hibadh	1.1	0.03	3-hydroxyisobutyrate dehydrogenase	BC003914	
Prdx4	1.1	0.02	peroxiredoxin 4	NM_016764	
Tsta3	1.1	0.04	tissue specific transplantation antigen P35B	NM_031201	
Lisch7	1.1	0.04	liver-specific bHLH-Zip transcription factor	BC004672	
Cryzl1	1.1	0.03	crystallin, zeta (quinone reductase)-like 1	BC010479	
Cox7a2	1.1	0.01	cytochrome c oxidase, subunit VIIa 2	NM_009945	
Ndufa1	1.1	0.04	NADH dehydrogenase 1 alpha subcomplex, 1	NM_019443	
Acadm	1.1	0.03	acetyl-Coenzyme A dehydrogenase, medium chain	NM_007382	
Pecr	1.1	0.02	peroxisomal trans-2-enoyl-CoA reductase	NM_023523	
Coq6	1.0	0.03	coenzyme Q6 homolog	BC024135	
Ndufs3	1.0	0.02	NADH dehydrogenase Fe-S protein 3	BC027270	
Sdhb	1.0	0.01	succinate dehydrogenase complex, subunit B	BC013509	
Adhfe1	1.0	0.02	alcohol dehydrogenase, iron containing, 1	BC026584	
Cyp51	1.0	0.00	cytochrome P450, 51	NM_020010	
Prdx1	1.0	0.03	peroxiredoxin 1	NM_011034	
Dhrs7	1.0	0.05	dehydrogenase/reductase 7	AK009385	
Grhpr	1.0	0.01	glyoxylate reductase/hydroxypyruvate reductase	NM_080289	
Ndufv1	1.0	0.01	NADH dehydrogenase flavoprotein 1	NM_133666	
Pdhb	1.0	0.02	pyruvate dehydrogenase beta	AK011810	
LOC14433	1.0	0.00	glyceraldehyde-3-phosphate dehydrogenase	NM_008084	
Ndufa7	-1.0	0.04	NADH dehydrogenase 1 alpha subcomplex, 7	NM_023202	
Sod2	-1.0	0.02	superoxide dismutase 2, mitochondrial	NM_013671	
Ndufa7	-1.0	0.01	NADH dehydrogenase 1 alpha subcomplex, 7	NM_023202	
Hsd17b12	-1.0	0.01	hydroxysteroid (17-beta) dehydrogenase 12	AK012103	
Glud	-1.0	0.01	glutamate dehydrogenase	NM_008133	
Dhodh	-1.0	0.01	dihydroorotate dehydrogenase	NM_020046	
Ndufa9	-1.0	0.05	NADH dehydrogenase 1 alpha subcomplex, 9	NM_025358	
Hsd17b12	-1.0	0.00	hydroxysteroid (17-beta) dehydrogenase 12	AK012103	
Bckdha	-1.1	0.01	branched chain ketoacid dehydrogenase E1alpha	NM_007533	
Glud	-1.1	0.02	glutamate dehydrogenase	NM_008133	
Recql4	-1.1	0.01	RecQ protein-like 4	NM_058214	
Decr1	-1.1	0.04	2,4-dienoyl CoA reductase 1, mitochondrial	NM_026172	
Ndufab1	-1.1	0.03	NADH dehydrogenase 1, alpha/beta subcomplex, 1	AK010307	
Uqcrfs1	-1.1	0.02	ubiquinol-cytochrome c reductase, Rieske iron-sulfur 1	AK003966	
Adh5	-1.1	0.02	alcohol dehydrogenase 5, chi	NM_007410	
Ndufa4	-1.1	0.04	NADH dehydrogenase 1 alpha 4	BC011114	
Cox5b	-1.1	0.04	cytochrome c oxidase, subunit Vb	NM_009942	
Prdx4	-1.1	0.05	peroxiredoxin 4	NM_016764	
Impdh2	-1.1	0.02	inosine 5'-phosphate dehydrogenase 2	M33934	
Ndufs1	-1.1	0.03	NADH dehydrogenase Fe-S protein 1	BC006660	
Ldh1	-1.1	0.03	lactate dehydrogenase 1, A chain	NM_010699	
Fzd7	-1.2	0.04	frizzled homolog 7	NM_008057	
Akr1b3	-1.2	0.05	aldo-keto reductase 1B3	NM_009658	
Mthfd1	-1.2	0.04	methylenetetrahydrofolate dehydrogenase	NM_138745	
Prdx2	-1.2	0.05	peroxiredoxin 2	NM_011563	

[1] All footnotes from Table S2 are applicable to Table S3.

Bondareva et al., 2007, Fig. S1

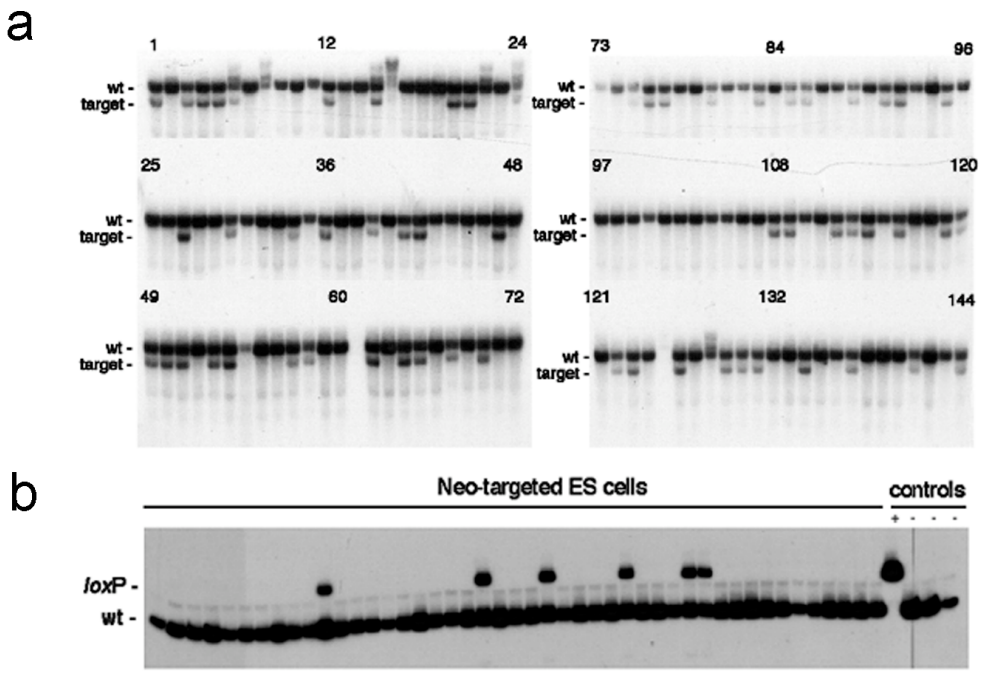

Bondareva et al., 2007. FIG S2